Automated image analysis techniques for cardiovascular magnetic resonance imaging
Geest, R.J. van der

Citation
Geest, R. J. van der. (2011, March 22). *Automated image analysis techniques for cardiovascular magnetic resonance imaging*. Retrieved from https://hdl.handle.net/1887/16643

CHAPTER

6

Evaluation of a new method for automated detection of left ventricular boundaries in time series of magnetic resonance images using an active appearance motion model

ABSTRACT

The purpose of this study was the evaluation of a computer algorithm for the automated detection of endocardial and epicardial boundaries of the left ventricle in time series of short-axis MR images based on an Active Appearance Motion Model (AAMM). In twenty short-axis MR exams, manual contours were defined in multiple temporal frames (from end-diastole to end-systole) in multiple slices from base to apex. Using a leave-one-out procedure, the image data and contours were used to build twenty different AAMM's giving a statistical description of the ventricular shape, gray value appearance and cardiac motion patterns in the training set. Automated contour detection was performed by iteratively deforming the AAMM within statistically allowed limits until an optimal match was found between the deformed AAMM and the underlying image data of the left-out subject. Global ventricular function results derived from automatically detected contours were compared to results obtained from manually traced boundaries. The AAMM contour detection method was successful in 17 out of 20 studies. The three failures were excluded from further statistical analysis. Automated contour detection resulted in small, but statistically non-significant, underestimations of ventricular volumes and mass: differences for end-diastolic volume were 0.3±12.0%, for end-systolic volume 2.0±23.4% and for left ventricular myocardial mass 0.73±14.9% (mean±SD). An excellent agreement was observed in the ejection fraction: difference of 0.1±6.7%. In conclusion, the presented fully automated contour detection method provides assessment of quantitative global function that is comparable to manual analysis.

Chapter

6

6.1 INTRODUCTION

Accurate quantification of left ventricular (LV) dimensions is important in the diagnosis of cardiac pathologies and the monitoring of the effect of treatment in various cardiac diseases. Cardiac magnetic resonance imaging allows accurate and reproducible measurements of global LV dimensions such as the end-diastolic (ED) and end-systolic (ES) chamber volumes, the ejection fraction and LV mass[1,2]. The introduction of Steady State Free Precession (SSFP) imaging techniques has resulted in significantly improved endocardial boundary definition, especially in regions of low flow, which were often poorly visualized by the older MRI techniques[3-5]. It has been shown that the SSFP yields an improvement of intra- and interobserver agreement in the assessment of global ventricular parameters when using manually traced myocardial boundaries[6]. Additionally, it was shown that SSFP yields better performance of automated contour detection software[6].

Despite these technical advances in MR pulse sequence development, quantification of the ventricular function parameters is still very much reliant on manual tracing of endocardial and epicardial contours in a large number of images. This post processing procedure adds a significant amount of time to the MR examination and leads to intra- and interobserver variabilities. Recently the concept of Active Appearance Models was introduced as a new framework for automated detection of object boundaries in images[7]. In previous studies we have adapted this AAM technique for the detection of LV and RV contours in 2D images. In the current work we extended the AAM method to operate on temporal sequences of short-axis images acquired using SSFP MRI.

The purpose of the present study was to develop and validate a new automated method for the detection of endocardial and epicardial contours in temporal sequences of short-axis MR images. The proposed method is training-based: it uses available time-series of images with expert drawn contours to build a statistical model of the shape, motion pattern and appearance (gray value in the images) of the left ventricle in time-sequences as seen in short-axis MR images. Once trained on a sufficiently large set of patient data, the statistical model is used to automatically find the cardiac boundaries in new image series. During this step the gray value information in a complete temporal sequence of images from end-diastole to end-systole is used, which guarantees that the method finds a consistent time-continuous segmentation result over the time-sequence. The results of automated contour detection were compared to results derived from manual contour tracings.

6.2 METHODS

6.2.1 Study Population

Eighteen cardiac patients (14 male, 4 female) and two healthy volunteers (all male) without history of cardiac disease were recruited for the study. The mean age of the subjects was 56 years (range 16–76) and mean weight 97 kg (range 54–150). The patients suffered from several pathologies including heart failure (n=8), hypertrophic cardiomyopathy (n=4), transplant follow-up (n=3), chest pain or angina (n=3). All study subjects gave written informed consent to participate in this study.

6.2.2 Magnetic Resonance Imaging

Patients and volunteers underwent MR imaging using a 1.5 T MR system (Sonata; Siemens Medical Systems, Erlangen, Germany). After localizing planes were obtained, a stack of short-axis images was acquired covering the complete left ventricle from apex to base using imaging sections of 6 mm thickness and an inter-section gap of 4 mm. MRI scanning parameters were as follows: TR=3.1 ms, TE=1.6 ms, flip angle=55°, receiver bandwidth=930 Hz/pixel, matrix size=192×256 and FOV=262×350 mm^2.

Chapter

6

6.2.3 Automated Contour Detection Algorithm

Introduction to Active Appearance Models

The newly developed automated contour detection algorithm presented in this paper is based on Active Appearance Models (AAM)[8]. An AAM is a statistical model that can be used to describe the appearance of short-axis MR images, including its typical variations, derived from a training set of example images. In the training set of images, the definition of the cardiac boundaries needs to be available via manually defined contours. An AAM consists of the mean appearance and a number of eigenvariations, which describe the variation in image appearance in the training set. Appearance in this context is a combination of the shape of the ventricle as seen in short-axis images and the gray value information contained in an MR image. For application of an AAM for detection of the LV contours only an image patch containing the LV plus its close surroundings is included in the AAM. By deforming the mean appearance along the eigenvariations, new 'realistic' cardiac MR images can be generated which were not included in the training set, but which are plausible in a statistical sense. To use an AAM for contour detection in cardiac MR images, this deforming procedure is applied to find an optimal match between the deformed AAM and the underlying image. The matching criterion used in our application was the

root-mean-square difference between the image pixels of the MR image and the model synthesized image.

Extension of AAM with Motion Information: AAMM

In previous work we have demonstrated the usefulness of AAM contour detection for the segmentation of the left and right ventricular boundaries in short-axis MR images[7]. This particular algorithm was limited to single two-dimensional images and the validity of the method was demonstrated on mid-ventricular end-diastolic images only. In this work an extension of the AAM contour detection was developed which performs modeling and contour detection for complete time-series of short-axis MR images. Since the method also includes information about the cardiac motion of the left ventricle, the method is called an Active Appearance Motion Model (AAMM). The rationale for this new approach is that we hypothesize that by modeling the image information contained in a time-series of images, the automated segmentation procedure will be more robust since all image data are employed during the detection procedure. By its nature, the segmentation result using AAMM contour detection will represent a time-continuous deformation of the endocardial and epicardial boundaries.

To apply AAMM contour detection for the detection of endocardial and epicardial contours in short-axis MR image series two steps need to be carried out:
1. Building an AAMM using available image data with manually defined expert contours;
2. Matching an AAMM to a new time-series of images by deforming the AAMM until it fits on the image data.
These two procedures are explained in more detail in the following sections.

Building an Active Appearance Motion Model

In the AAMM, the appearance of the left ventricle is modeled for the systolic phase of the cardiac cycle by considering the image frames from ED to ES. An image sequence is normalized to a fixed number of frames T (6) using a nearest neighbor interpolation, so that the ED and ES frames map to the same frame number (1 and 6, respectively). In the training set the endocardial and epicardial contours are defined manually by an independent expert. In each time frame, the image appearance of the left ventricle is modeled as an appearance vector describing the pixel intensity values in an image patch spanned by the manual contour. The vectors for shape points and image patch intensities for each time frame are

concatenated and ordered according to their phase number (1-6). Only imaging sections in which the left ventricular myocardium was visualized for the full circumference in all image frames, were included in the model. Therefore, often one basal and in a few cases an apical section needed to be excluded from the training set of image series. By applying a Principal Component Analysis on the training samples the mean and the most characteristic eigenvariations (modes of variation) of appearance vectors are derived. The resulting AAM describes the average motion pattern that is associated with the cardiac contraction as seen in short-axis cardiac MR images, including the most characteristic anatomical and functional variations in the cardiac cycle (Figure 6-1). In the current implementation no distinction was made between slice levels: apical, mid and basal slices were combined in a single model.
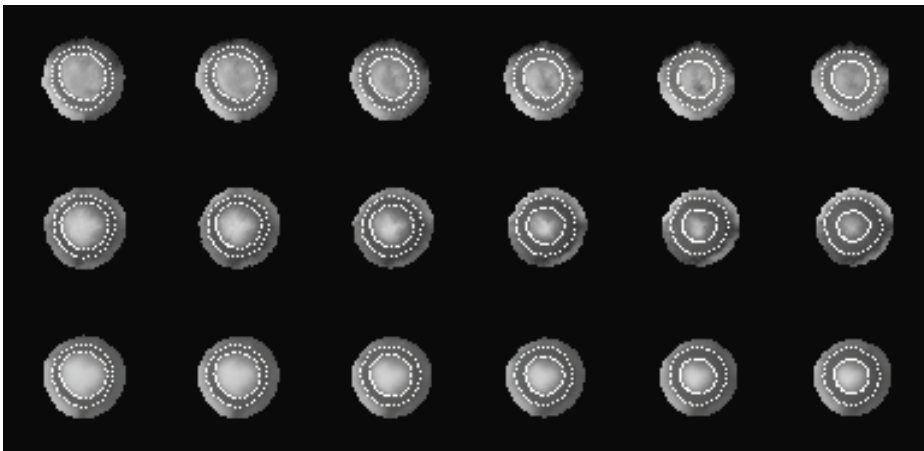

Figure 6-1. Illustration of a trained AAMM with the most important modes of variation. The top row shows the average appearance of the systolic contraction from ED to ES as seen in the short-axis MR images used to construct the AAMM. The middle and bottom rows illustrate the most significant mode of variation represented by the average AAMM plus or minus three times the standard deviation, respectively.

Matching an Active Appearance Motion Model

For each study the only manual interaction required is the definition of the ES time frame; the first time frame is assumed to represent ED. The AAMM is then positioned at the center of the LV using an automatically detected LV center point[9]. For each slice location, six evenly spaced frames from ED to ES are processed simultaneously. Contour detection is performed by automatically adjusting the AAMM parameters until the best fit is found between the deformed AAMM and the underlying image data using an iterative procedure. In the first few iterations the pose of the average appearance is modified using translation, rotation and scaling. In the

following iterations the appearance is modified by changing the AAMM parameters within ±3 standard deviations. This iterative process continues until a minimum gray value difference (expressed as the root mean square error) is obtained between the model and the six time frames. The matching process results in the endocardial and epicardial contours for all six time frames.

Figure 6-2. (A) Example of a time series of images from ED to ES with manually defined endocardial and epicardial contours (top rows). The endocardial contours are traced around the trabeculations and papillary muscles, which results in a time-continuous motion pattern of the endocardial boundary. (B) Automatically detected contours generated by the AAMM contour detection method. The contours are comparable to the manually traced boundaries illustrated in (A).

6.2.4 Manual analysis

Experienced observers manually traced endocardial and epicardial contours in all cardiac phases and all slice levels in which the myocardium was visualized. Four observers performed the contour tracing, each of them analyzing five exams. The endocardial boundaries were traced around the trabeculations and papillary muscles such that a smooth convex-shaped endocardial contour resulted that exhibits a time-continuous deformation over the cardiac cycle (Figure 6-2A). Epicardial contours were traced at the outer boundary of the myocardium inside epicardial fat when present. Images at the base of the heart showing myocardium for less than 50 percent along its circumference were excluded from analysis. To avoid inconsistencies in image interpretation between observers, one of the observers reviewed all segmentation results and made adjustments to the contours if deemed necessary. In ten randomly chosen subjects manual tracing was carried out by a second observer to assess inter-observer variability. The quantitative ventricular function results derived from the manual tracings served as gold standard.

6.2.5 Comparison between Automatically and Manually Defined Contours

Chapter

6

For evaluation of the performance of the AAMM contour detection methods a leave-one-subject-out approach was used. For each study subject automated detection was carried out using an AAMM that was trained on the remaining nineteen subjects. LV volumes were assessed from the available contours using Simpson's rule. The quantitative global ventricular function results derived from the automatically detected contours were compared to the results derived from manual contour tracings. The following parameters were included in this comparison: EDV, ESV, EF and LV mass. EDV was defined as the volume of the LV in the first time frame; ESV was defined as the smallest volume of the LV; EF was defined as $100\% \times (EDV-ESV)/EDV$ and LV mass was assessed as the average volume of the myocardium in the ED and ES phases multiplied by the specific density of myocardial tissue (1.05 g/ml). For each parameter the agreement between manual and AAM results was analyzed by computing the mean and standard deviation of the paired differences.

6.3 STATISTICAL ANALYSIS

Values are expressed as mean ± SD. The paired Student t-test was used to assess statistical significance of the differences for each parameter between manual and automated analysis. A p-value<0.05 was considered statistically significant. Parameters obtained by manual and automated analysis were compared using linear regression analysis and by calculating

absolute and relative differences between methods according to the methods of Bland and Altman[10].

Table 6.1. Global ventricular function parameters derived from manually defined contours.

Parameter	Mean	SD
EDV (ml)	161	86
ESV (ml)	104	95
EF (%)	46	19
LVM (g)	126	52

EDV: End-diastolic volume; ESV: End-systolic volume; EF: Ejection fraction; LVM: Left ventricular mass (average of ED and ES values)

6.4 RESULTS

6.4.1 Manual Analysis Results

The number of slices included per study varied between 4 and 9 (average 6.7; SD 1.2). The phase number of ES varied between 6 and 10 (average 7.7; SD 1.3). Endocardial and epicardial contours were manually traced in the slices covering the left ventricle in the phases from ED to ES, resulting in contour tracings in 1010 images. Global function results derived from the manual tracings are summarized in Table 6-1. The interobserver variabilities for EDV were 3.1 ± 4.8% for ESV 2.4 ± 14.8%, for EF 2.9 ± 7.2% and for LVM 2.1±8.7% (Table 6-2). Limits of agreement between two observers using manual analysis for EDV were between −6.5% and +12.7%; for ESV between −27.2% and +32%; for EF between −11.5% and +17.3% and for LVM between −15.3% and +19.5%.

Table 6.2. Interobserver variability for quantification of global LV parameters using manual contour tracing.

Parameter	Obs1-Obs2 (abs)	Obs1-Obs2 (%)
EDV	4.2 ± 7.7 ml	3. ± 4.8%
ESV	0.5 ± 6.7 ml	2.4 ± 14.8%
EF		2.9 ± 7.2%
LVM	2.2 ± 9.0 g	2.1 ± 8.7%

EDV: End-diastolic volume; ESV: End-systolic volume; EF: Ejection fraction; LVM: Left ventricular mass (average of ED and ES values)

6.4.2 AAM contour detection

The twenty available studies were used to generate 20 different AAMM models, in each model the image data of one subject was left out and the corresponding AAM model was used for the automated detection of the left-out subject. Figure 6-1 gives an example of an AAMM model. It shows the average appearance of the systolic contraction in a short-axis MR image, including the first two most significant modes of variation. Figure 6-2B shows an example of automated contour detection results for a mid-ventricular time series of images. The contours detected are very similar to the manually drawn contours for this series shown in Figure 6-2A.

Automated AAMM contour detection was performed successfully in 17 out of twenty exams. In three studies the automated contour detection procedure failed to converge to a correct segmentation result. Visual inspection of these three studies revealed distinct features not seen in any of the other exams:

1. In one exam a bright rim of pericardial fluid (thickness 4-6 mm) was seen at the lateral wall;
2. The second study was a patient with a severely dilated ventricle with a thin ventricular wall and low ejection fraction (EDV 290 ml, average ED wall thickness 5.9 mm, EF 11%)
3. The third study was a patient with severe hypertrophic cardiomyopathy. (LV mass 252 g, local ED septal wall thickness of 26 mm; EF 79%).

Chapter

6

The results of these three studies were excluded from the statistical analysis. For the remaining 17 studies the comparative results between global functions measurements obtained by either manual contour tracing and automated contour detection are listed in Table 6-3. For all the parameters, the differences were found to be statistically non-significant. Linear regression analysis demonstrated an excellent linear correlation between methods with r-values ranging from 0.96–0.99 (p<0.01). Bland-Altman plots comparing the manually obtained and automatically obtained global function parameters are presented in Figure 6-4. In these plots the differences between the methods are displayed as relative errors. There was a very small statistically non-significant bias of the automatically determined parameters. The bias for the global function parameters was never higher than 2%. The 95% limits of agreement for the assessment of global function parameters using AAM contour detection compared to manual analysis were for EDV between −23.8 and +23.3%; for ESV between -43.8% and +47.8%; for EF between 13.0 and +13.3%; and for LVM between -28.5 and +29.9%. In Figure 6-4 a graphical presentation is

given of the differences between automated and manual analysis and observer variabilities using manual analysis.

Computation time for the detection of contours in a complete time sequence of images from ED to ES was less than 3 seconds using a 1GHz PC operating under the Linux operating system. The total computation time for all slices from apex to base was less than 20 seconds per examination.
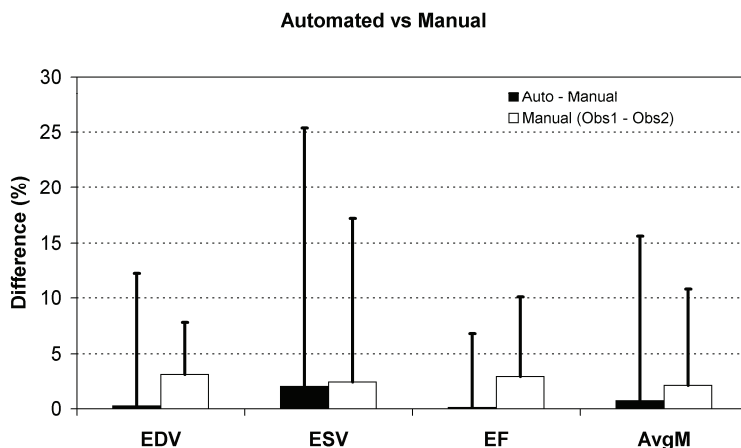
Automated vs Manual

Figure 6-3. Graphical presentation of error of automated contour detection (using manual traced contours as the reference) compared with interobserver variability for manual contour tracing. The error bar shows the standard deviation of the paired differences between measurements for the given global function parameters. Abbreviations: EDV: end-diastolic volume; ESV: end-systolic volume; EF: ejection fraction; LVM: left ventricular mass (average of ED and ES values).

6.5 DISCUSSION

Automated contour detection is a prerequisite for time-efficient quantification of left ventricular function from multi-slice short-axis cine MR imaging studies. Developing of an accurate and robust detection algorithm is a challenging problem due to large variations in patient characteristics and features present in the images. It requires knowledge about the MR image sequence used and knowledge about the anatomy of the heart and neighboring structures. Only trained observers are capable to reliably and reproducibly trace the myocardial contours. It is often helpful to visualize the images in a cine mode to correctly interpret the structures seen in the images. When image information is unreliable or inconclusive, the final judgment is based on a model derived from previous experience.

Table 6-3. Global function results obtained by either manual or automated contour detection. Only those exams are included in which the AAMM contour detection converged to a valid match.

	EDV		ESV		EF		LV mass	
	Manual	**Auto**	**Manual**	**Auto**	**Manual**	**Auto**	**Manual**	**Auto**
1	63	71	24	31	63	57	57	43
2	171	183	121	118	29	36	147	139
3	142	135	91	82	36	39	102	104
4	81	60	39	23	52	62	90	109
5	109	125	33	43	70	66	142	169
6	209	207	140	154	33	26	145	125
7	77	77	34	34	56	56	62	49
8	72	63	38	30	47	52	47	56
9	112	114	52	43	54	62	105	131
10	173	157	94	85	46	46	123	134
11	143	143	54	62	62	57	136	121
12	300	329	217	281	28	15	217	210
13	160	175	104	115	35	34	98	105
14	146	148	81	69	44	53	121	114
15	127	138	54	53	58	61	120	126
16	127	145	64	80	50	45	96	96
17	418	408	336	361	20	11	225	221
Mean	**155**	**157**	**93**	**98**	**46**	**46**	**120**	**121**
SD	**89**	**91**	**80**	**92**	**14**	**17**	**49**	**49**

EDV: End-diastolic volume; ESV: End-systolic volume; EF: Ejection fraction; LVM: Left ventricular mass (average of ED and ES values)

Chapter

6

The presented AAMM contour detection technique is trained using previously obtained MR imaging studies with expert drawn contours. The generated AAMM contains information about the shape of the left ventricle, the motion and deformation pattern of the left ventricle and the gray value distribution in MR images. By restricting the deformation of the AAMM to statistically defined limits, each deformed AAMM represents a plausible segmentation result. Therefore, the detection algorithm uses similar a-priori knowledge as a human observer. Since the contour detection is based on the minimization of the gray value difference between the actual image data of a whole time-series of images and the deformed representation of the AAMM, the method is relatively insensitive to false edges present in the

images. This is in contrast to other contour detection approaches which rely on local image features such as gray value edges[9,11,12]. An additional advantage of the presented automated method is that it exploits all image information contained in a time-series of images during detection of the contours. This is in accordance with how manual tracing is carried out, since often images are displayed in a cine-mode in order to correctly and consistently interpret the structures seen in the images. Basic physiology dictates that myocardial motion and deformation of the ventricular wall should constitute a time-continuous pattern. The presented algorithm fulfills this constraint since the detected myocardial boundaries are smooth and represent a time-continuous pattern.

The contour detection method was evaluated on clinical cases from various cardiac pathologies. Within the study population the ejection fraction ranged from 11% - 66%; the LV mass ranged from 43 g - 221 g. Nevertheless, automated contour detection provided global ventricular function results comparable to results obtained by manual analysis. No statistically significant differences were found between results obtained by manual and automated analysis. With a processing time of less than 20 seconds for an examination, the contour detection method was proven to be time efficient. Since user interaction was limited to manually defining the ES time frame, observer bias is expected to be very much limited.
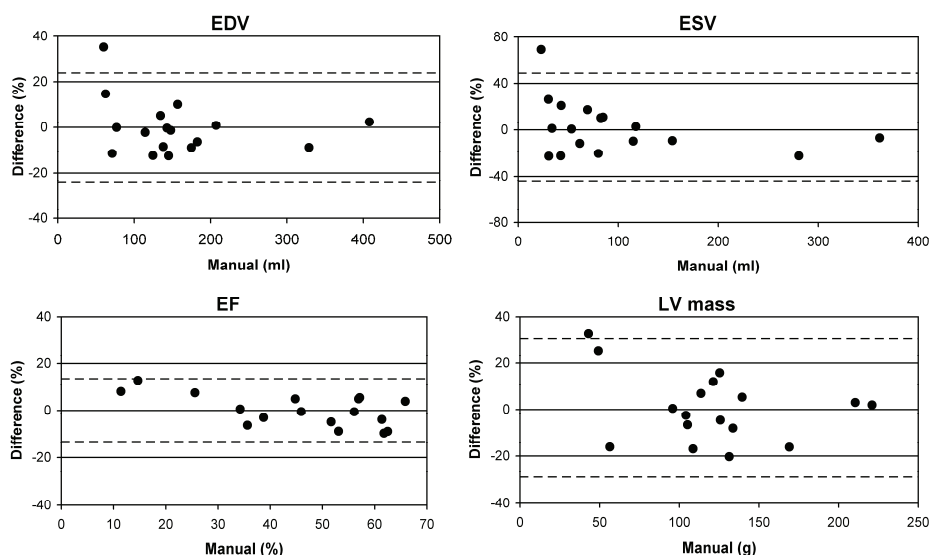

Figure 6-4. Bland-Altman plots for EDV, ESV, EF and left ventricular mass.

6.5.1 Limitations

This study has a number of limitations. In three MR examinations the automated contour detection was unable to detect reliable contours. Inspection of these examinations revealed that in each of these studies distinct features were present not seen in the other studies. Therefore, the correct segmentation for those studies could not be obtained by deforming the AAMM. The occurrence of these failures stresses the importance of using a sufficient number of representative MR studies for training the AAMM. It is assumed that by increasing the number of studies to train the AAMM, the descriptive power of the model increases and the failure rate will be reduced considerably. Currently we have not yet studied the optimal size of the training set and the optimal distribution of various pathologies within the training set.

The current implementation of the method can only be applied to imaging slices where a complete circumference of myocardium is present in all time-frames. In most patients, this condition is not fulfilled for the most basal slice location of the ED frame, since due to through-plane motion during the systolic phase, the myocardial tissue seen in the ED phase may move out of the imaging plane during contraction. Therefore, some imaging sections could not be evaluated using the proposed contour detection method. A possible solution for this problem could be to use a single-phase AAM for the most basal imaging section of the ED phase, as presented by Mitchell at al[7].

Chapter

6

6.5.2 Future studies

To further investigate the strengths and limitations of the presented AAMM contour detection technique and to explore possibilities to improve the method, further studies are required. As already mentioned, it is needed to collect additional clinical MR exams with manually drawn contours to investigate the optimal size for the AAMM training set. Additionally, it is relevant to study whether clinical data of patients with different pathologies should be incorporated in a single model, or whether it proves more successful to have separate models for specific pathologies. A similar question arises when it comes to inclusion of image data acquired with slightly different imaging protocols, or even images obtained from different MR systems in a single model or separate models. In the three cases that were excluded from statistical analysis, distinct features were present explaining why the AAMM contour detection did not perform successfully. However, to understand the sources of the differences between AAMM and manual contour detection in the remaining 17 subjects, further investigation into the sources of these differences are warranted.

Table 6.4. Comparison between manual and automated global function results for those examinations in which the AAMM contour detection converged to a valid match (n=17).

	Auto – Man (abs)	Auto - Man (%)
EDV	-2.9 ± 13.2 ml	-0.3 ± 12.0%
ESV	-5.1 ± 18.9 ml	-2.0 ± 23.4%
EF		0.1 ± 6.7%
LVM	-1.2 ± 14.1 g	-0.7 ± 14.9%

EDV: End-diastolic volume; ESV: End-systolic volume; EF: Ejection fraction; LVM: Left ventricular mass (average of ED and ES values)

6.6 CONCLUSION

A fully automated contour detection method is presented which provides quantitative indices of global function that are comparable to manual analysis. The method can be applied to images acquired with different MR systems and pulse sequences by retraining the AAMM using MR images with expert drawn contours available. Further studies are needed to establish the optimal size and distribution of patients with varying cardiac pathologies in the training set used to build the AAMM.

6.7 REFERENCES

1. Higgins, CB, Sakuma, H. Heart disease: functional evaluation with MR imaging. Radiology 1996; 199:307-315.
2. Semelka RC, Tomei E, Wagner S, Mayo J, Kondo C, Suzuki J, Caputo GR, Higgins CB. Normal left ventricular dimensions and function: Interstudy reproducibility of measurements with cine MR imaging. Radiology. 1990; 174: 763-768.
3. Carr JC, Simonetti O, Bundy J, Li D, Pereles S, Finn JP. Cine MR angiography of the heart with segmented true fast imaging with steady-state precession. Radiology. 2001; 219:828-834.
4. Barkhausen, J, Ruehm, SG, Goyen M, Buck T, Laub G, Debatin JF. MR Evaluation of Ventricular Function: True Fast Imaging with Steady-State Precession versus Fast Low-Angle Shot Cine MR Imaging: Feasibility Study. Radiology. 2001; 219: 264-269.
5. Lee VS, Resnick D, Bundy JM, Simonetti OP, Lee P, Weinreb JC. Cardiac function: MR evaluation in one breath hold with real-time True Fisp imaging with steady-state precession. Radiology. 2002; 222;835-842.
6. Plein S, Bloomer TN, Ridgeway JP, Jones TR, Brainbridge GJ, Sivananthan MU. Steady-state free precession magnetic resonance imaging of the heart: Comparison with segmented K-space gradient-echo imaging. J Magn Reson Imaging. 2001; 14:230-236.
7. Mitchell SC, Lelieveldt BPF, van der Geest RJ, Bosch JG, Reiber JHC, Sonka M. Multistage hybrid active appearance model matching: Segmentation of left and right ventricles in cardiac MR images. IEEE Trans Med Imaging. 2001; 20:415-423.

8. Cootes TF, Beeston C, Edwards GJ, Taylor CJ. A unified framework for atlas matching using active appearance models. Proc.Information Processing in Medical Imaging 1999, Lecture Notes in Computer Science. 1999: 1613:322-333.
9. van der Geest RJ, Buller VGM, Jansen E, Lamb HJ, Baur LHB, van der Wall EE, de Roos A, Reiber JHC. Comparison between manual and automated analysis of left ventricular volume parameters from short axis MR images. J Comput Assist Tomogr. 1997; 21:756-765.
10. Bland JM, Altman DG. Statistical methods for assessing agreement between two methods of clinical measurement. Lancet. 1986; 8:307-310.
11. Baldy C, Doueck P, Croisille P, Magnin IE, Revel D, Amiel M. Automated myocardial edge detection from breath-hold cine-MR images: evaluation of left ventricular volumes and mass. Magn Reson Imaging. 1994; 12:589-598.
12. Lalande A, Legrand L, Walker PM, Guy F, Cottin Y, Roy S, Brunotte F. Automatic detection of left ventricular contours from cardiac cine magnetic resonance imaging using fuzzy logic. Invest Radiol. 1999; 34:211-217.

Chapter

6